The size distribution of chemical elements of atmospheric aerosol at a semi-rural coastal site in Venice (Italy). The role of atmospheric circulation

Mauro Masiol;Stefania Squizzato;Daniele Ceccato;Bruno Pavoni

Published in Chemosphere 119 (2015) 400–406

DOI: http://dx.doi.org/10.1016/j.chemosphere.2014.06.086

The size distribution of chemical elements of atmospheric aerosol at a semi-rural coastal site in Venice (Italy). The role of atmospheric circulation

Mauro Masiol[a,†], Stefania Squizzato[a (*)], Daniele Ceccato[b,c], Bruno Pavoni[a]

[a] Dipartimento di Scienze Ambientali, Informatica e Statistica, Università Ca' Foscari Venezia, Dorsoduro 2137, 30123 Venice, Italy

[b] Dipartimento di Fisica e Astronomia "Galileo Galilei", Università degli Studi di Padova, Via Marzolo 8, 35100 Padua, Italy

[c] Laboratori Nazionali di Legnaro, Istituto Nazionale di Fisica Nucleare, Viale dell'Università 2, 35020 Legnaro, Italy

[†] Now at: Division of Environmental Health & Risk Management, School of Geography, Earth & Environmental Sciences, University of Birmingham, Edgbaston, Birmingham B15 2TT, United Kingdom

Corresponding author:

Stefania Squizzato; E-mail: stefania.squizzato@unive.it

Dipartimento di Scienze Ambientali, Informatica e Statistica, Università Ca' Foscari Venezia, Dorsoduro 2137, 30123 Venice, Italy

Tel: +39 041 2348639

Abstract

The concentrations of selected elemental tracers were determined in the aerosol of a semi-rural coastal site near Venice (Italy). Size-segregated aerosol samples were collected using an 8-stage cascade impactor set at 15 m above ground, during the cold season (late autumn and winter), when high levels of many pollutants are known to cause risks for human health. From the experimental data, information was extracted on potential pollutant sources by investigating the relationships between elements in the different size fractions. Moreover, an approach to highlight the importance of local atmospheric circulation and air mass origin in influencing the PM composition and fractional distribution is proposed.

Anthropogenic elements are strongly inter-correlated in the submicrometric (< 1 μm) (S, K, Mn, Cu, Fe and Zn) and intermediate mode (1-4 μm) (Mn, Cu, Zn, Ni) and their relationships highlight the presence of several sources (combustions, secondary aerosol, road traffic). In the intermediate mode, associations having geochemical significance exist between marine (Na,Cl and Mg) and crustal (Si, Mg, Ca, Al, Ti and K) elements. In the coarse mode (> 4 μm) Fe and Zn are well correlated and are probably linked to tire and brake wear emissions.

Regarding atmospheric circulation, results show increasing levels of elements related to pollution sources (S, K, Mn, Ni, Cu, Zn) when air masses come from Central and Eastern Europe direction and on the ground wind blows from NWN-N-NE (from mainland Venice). Low wind speed and high percentage of wind calm hours favor element accumulation in the submicrometric and intermediate modes. Furthermore, strong winds favor the formation of sea-spray and the increase of Si in the coarse mode due to the resuspension of sand fine particles.

Keywords: Element mass size distributions; PIXE analysis; Lagoon of Venice; Meteorological conditions

1. Introduction

Airborne particulate matter (PM) plays direct (Yu et al., 2006) and indirect (Lohmann and Feichter, 2005) effects on climate, affects visibility (Chow et al., 2002), enters in many chemical reactions in the atmosphere (Buseck and Schwartz, 2003; Kroll and Seinfeld, 2008; George and Abbatt, 2010) and may cause a number of adverse effects on human health (Pope et al., 2009). The dimension of particles is directly related to their emission sources, as mechanically generated particles (e.g., wind-blown dust, sea spray) are generally larger than 1 μm, whereas combustion-generated particles (high-temperature processes, traffic exhausts, many industrial activities) are smaller than 1 μm (e.g., Lewis and Schwartz, 2004; Seinfeld and Pandis, 2006; Ning and Sioutas, 2010).

The present study has been conducted in Venice, located in the eastern part of the Po Valley (Italy), one of the most polluted areas in Europe (EEA, 2013) and it is influenced by both mainland anthropogenic emissions (automotive traffic, shipping emissions, industrial processes) (Rampazzo et al., 2008a; Rampazzo et al., 2008b, Contini et al., 2011), secondary aerosol formation (Squizzato et al., 2013) and natural sources such as sea spray from the near Adriatic Sea and crustal material (Masiol et al., 2012a).

However, the air quality in Venice has also been shown to be very sensitive to local atmospheric circulation patterns (Masiol et al., 2010; 2012a). Furthermore, PM pollution was associated with external transports from the continental Europe and the Po Valley. These studies reported that PM pollution increases when air masses originate in Central Europe and secondary sulfates build up when air masses pass over the Po Valley (Squizzato et al., 2012). On the contrary, air masses coming from Northern Europe were shown to have a cleaning effect.

Recently, Toscano et al. (2011) reported the size distribution of some selected elements in the aerosol of the Venetian Lagoon. Readings were taken at three sites characterized by different anthropogenic influences and particles with aerodynamic diameter less than 3 μm were predominant. Likewise, several studies were conducted in Europe (Salma et al., 2002; Samara and Voutsa, 2005; Karanasiou et al., 2007) and Italy (Rizzio et al., 1999) to investigate the elemental size distribution on different environmental scenarios (e.g. urban background, heavy traffic, roadside, tunnel and rural residential area). However, although the weather condition and the long distance transport are considered determining factors on size distributions (Samara and Voutsa, 2005) and in changing air quality in non-polluted areas (Rizzio et al., 1999), information is still lacking about the role of atmospheric circulation and long-range transport processes on the elemental mass size distributions.

In this study the mass size distributions of some elements recognized as tracers for specific sources of PM were investigated in a semi-rural coastal site near Venice (Italy). From experimental

data, information was extracted to identify the potential sources of PM and elements, by examining the relationships between elements in the different size fractions. Moreover, an approach to highlight the importance of local atmospheric circulation and air mass origin in determining the PM composition and fractional distribution is proposed. Data were processed in association with back-trajectories and local atmospheric circulation (wind speed and direction) to reveal significant links between atmospheric dynamics and aerosol elemental composition.

2. Materials and method

2.1 Sampling and analysis

A total of 112 individual sub-samples were obtained from 14 daily samples of aerosol, which were size-partitioned using an 8-stage single-orifice cascade impactor (14 daily samples x 8-stages=112 sub-samples) (model I-1, PIXE International Co., USA) as previously reported by Salma et al. (2002). The sampling station was located on a lighthouse (45.4227 N, 12.4368 E, 15 m above ground level) at the end of a 300 m-long dam at the Lagoon of Venice port channel of the Lido (Figure 1a). Prevalent winds during the sampling campaign flowed from N-NE (Figure 1b), i.e. from the sea, the Lagoon and agricultural environments. The experimental data were collected during the late autumn and winter (October 2007 - January 2008, non-breeze season), when the highest levels of both PM and many gaseous pollutants are generally observed (ARPAV, 2013).

The cascade impactor had 7 stages with nominal cut-points (d_{50}-values, and/or equivalent aerodynamic diameters) of 16, 8, 4, 2, 1, 0.5, 0.25 μm ahead of the backup filter (8 stages in total). The nominal flow rate was 1 L min^{-1}. Collection media were polycarbonate membranes (Prepared Ring with Nuclepore PR-1N, PIXE International Co., USA, pore size 0.4 μm, Ø 27 mm) coated with Vaseline to reduce particle rebound. Air flow was frequently monitored using a flow meter and manually adjusted to be consistent with the instrument margin of tolerance (±10%). After sampling, membranes were stored at −20 °C in clean Petri slides until analyses to avoid sample contamination, degradation and losses.

Samples were analyzed for major, minor and trace elements with atomic number ≥ 11 (Na, Mg, Al, Si, S, Cl, K, Ca, Ti, V, Cr, Mn, Fe, Ni, Cu, Zn) using the Particle Induced X-ray Emission (PIXE) experimental setup facility at the INFN Legnaro laboratories. The GUPIX code (Maxwell et al., 1995) was used to fit the X-ray energy spectra and to calculate the absolute elemental areal densities (ng cm^{-2}), their errors and the detection limit (DLs) values. The quality of the analytical results was assured by frequently analyzing the international reference material SRM 2783 (NIST, USA). Further details about sampling, analytical precision and limits of detection are available in supplementary material and in Table SI1.

2.2 Weather data and back-trajectory analyses

Wind speed and direction were measured hourly at a regional environmental protection agency station (ARPAV-Centro Meteorologico di Teolo), located about 6 km East of the sampling site (Figure 1). Moreover, daily back-trajectories were simulated and then clustered using the Hybrid Single-Particle Lagrangian Integrated Trajectory (HYSPLIT) model version 4 (96 hours backward, starting at 00:00, 6:00, 12:00 and 18:00 h local time, at 150 m above ground level, NCEP/NCAR Reanalysis data fields) (Draxler and Rolph, 2013; Rolph, 2013).

3. Results and discussion

Preliminary data evaluation and handling was carried out to clean up the dataset. Data with values below the DLs and/or with high percentage of error (> 50%) were substituted by DLs/2; casual and systematic contaminations were checked by a careful evaluation of field blanks. No anomalous data were detected. The total concentration of the analyzed elements, i.e. the sum of element concentrations in all stages, which represents total suspended particulate matter (TSP), is reported as a boxplot in Figure SI1. Basing on median values, sulfur is the most abundant element (746 μg m^{-3}), followed by Cl (491 ng m^{-3}), Ca (193 ng m^{-3}), K (183 ng m^{-3}) and Na (153 ng m^{-3}).

Each collected sample was then processed to represent the differential mass distributions with both histograms and lognormal distribution models (e.g. Majoral et al., 2006, and references therein). Figure 2 reports the average element size distribution as differential mass concentration. In most samples, only a few membranes designed to catch particles smaller than 0.25 μm (back-up filter) contained sufficient material to be measured accurately for most of the analyzed elements. Results show that Ti, Cl, Ni, Cu and Ca are more concentrated in the intermediate mode (range 1-4 μm), whereas sulfur, potassium, vanadium and manganese are mostly in the submicrometric range mode (< 1 μm). Other elements clearly show bimodal distributions (Na, Mg, Al and Cr) in both submicrometric and coarse ranges, whereas iron and zinc ranged from 0.25 to 4 μm. The similar intermediate mode for Na, Mg and Cl reveals the probable common origin from sea-water, whereas the presence of Na and Mg in the submicrometric mode may be due to anthropogenic sources as it was observed for Al and Mn as well. Ti and Si appear also enriched in the >16 μm diameter, but this was mainly due to a single sample with very high concentrations occurred in particular meteorological conditions. The role of atmospheric circulation will be discussed in the subsection 3.3.

From a comparison with previous studies (Rizzio et al., 1999; Salma et al., 2002; Samara and Voutsa, 2005; Karanasiou et al., 2007), the obtained distributions reproduce a general trend, showing the anthropogenic elements linked to the finest fraction and those soil related with the

coarse one. A more detailed comparison is difficult because of the different particle size classifications applied in the studies. In addition, the size distribution patterns vary significantly with the sampling location, reliability of the impactor, overloading and hydroscopicity of collection substrates, and weather conditions (Samara and Voutsa, 2005).

When combining each analyzed element with its most probable emission source, size distributions fitted well with their interpretations. Elements related to sea spray (Na, Cl, secondarily Mg) and mineral dust (Al, Si, Ca) exhibited evident modes in the super-micrometric fraction (> 1 μm), showing their natural origin from mechanical processes, i.e. breaking waves and soil/sediment deflation, respectively. Sulfur exhibited an evident peak between 0.25 and 0.5 μm, indicating its secondary origin from the nucleation of H_2SO_4, NH_3, and H_2O in the atmosphere (Seinfeld and Pandis, 2006; Benson et al., 2011). Moreover, sulfur showed an enrichment in correspondence to sea-salt tracers in samples with high values of marine components, clearly revealing their origin also from the seawater. An example of distribution for a marine aerosol enriched sample (TSP concentration very close to the seawater ratio: Na 639 ng m^{-3}, Cl 1068 ng m^{-3}) is reported as supplementary material (Figure SI2).

Vanadium, which is a well-known tracer for the transformation and combustion of fossil fuels and residue oil (e.g., Moreno et al., 2010) was frequently reported having a submicrometric mode in association with sulfur (0.25 and 0.5 μm) (Samara e Voutsa, 2005; Moldanová et al., 2009) and this was also observed in this study.

In comparison with a previous paper on aerosol elemental distributions carried out in the Venice area (Toscano et al., 2011), this study detects modes at smaller diameters for some elements related to natural origins such as sodium (sea-salt) and aluminum (crustal component) and to anthropogenic sources (Mn). This fact can be attributed to the difference in sampling sites and seasons. Further, samples were collected at a greater height (15 m above sea level) and at a site distant from anthropogenic contamination, whereas earlier study samples were collected at ground level and near potential emission sources. Despite this, similar concentrations have been detected, except for Mg that shows higher levels in this study. A comparison between the detected average concentrations is presented in Table SI2.

3.1 Correlations amongst the analyzed elements

Three main modes were evidenced for most samples (Figure 2), thus splitting the elements in three fractions: submicrometric (less than 1 μm, sum of the first two stages and back-up filter), intermediate (1-4 μm) and coarse (> 4 μm). The average elemental concentrations in each fraction are summarized in Table 1. An explorative analysis of the inter-relations of the original data in each

fraction was then performed using the Pearson's correlation *(r)*. Only fractions with at least two stages over the DLs were included in the computations. Significant correlations (p-value < 0.05 and N=number of samples >4) for each mode are reported as supplementary material (Table SI3).

Submicron-sized aerosol is usually attributed to high energy sources (i.e. combustions) or secondary aerosol formation processes. Sulfur, potassium, manganese and iron present the highest number of significant correlations among them, generally with titanium, copper and zinc ($r_{S/K}$=0.83; $r_{S/Mn}$=0.96; $r_{Mn/Fe}$= 0.83; $r_{Mn/Cu}$=0.98; $r_{Fe/Zn}$= 0.95). High correlations in this fraction may therefore represent elements related to anthropogenic sources or linked to external transports. Previous studies (Masiol et al., 2012b) indicate that in cold seasons an average percentage of 96% of total sulfur is in the form of sulfate, which is largely recognized as a main component of secondary ammonium sulfate aerosol. Potassium has been largely associated to biomass combustions (Saarnio et al., 2010), and secondarily to other combustion sources (e.g. waste incinerators and coal power plants). Manganese, iron, copper and zinc have also been associated to local pollution (Masiol et al., 2012a) mainly due to road traffic, as most of those elements are recognized as specific road dust components (Sternbeck et al. 2002; Amato et al., 2011; Pant and Harrison, 2013). Calcium is also related to these elements ($r_{Ca/Mn}$=0.58; $r_{Ca/Fe}$=0.63) probably due to the resuspension of small particles from road surface or to the construction work in the proximity of the sampling site.

In the intermediate mode, associations having geochemical significance exist between marine ($r_{Na/Cl}$ = 0.97; $r_{Na/Mg}$ = 0.97; $r_{Mg/Cl}$ = 0.99), crustal ($r_{Si/Mg}$ = 0.98; $r_{Ca/Mg}$ = 0.99; $r_{Si/Al}$ = 0.84; $r_{Al/Ti}$ = 0.96; $r_{K/Al}$ = 0.85; $r_{K/Ca}$ = 0.99) and anthropogenic elements ($r_{Mn/Cu}$ = 0.97; $r_{Mn/Zn}$ = 0.97; $r_{Ni/Cu}$= 0.90; $r_{Ni/Zn}$ = 0.89). The typical major crustal elements (Si, Al, Ca, K, and Mg) were associated to the mineral dust source, whereas Na, Cl and Mg were tracers for sea spray, according to the average compositions of the lithosphere and seawater, respectively. Manganese, zinc, copper and nickel were linked to various anthropogenic sources, such as traffic (Mn, Cu, Zn), as brake, tire and mechanic component wear and combustion processes (Ni). However, as many emission sources can release varying amounts of the same element or chemical compound into the atmosphere, some results may be difficult to interpret. Sodium and magnesium content, for example, can be found both in marine and crustal particles, manganese both in crustal and anthropogenic, sulfur both in crustal, marine and secondary sulfates, and so on.

In the coarse fraction, Si and Ti present the highest percentage. Ti shows a significant correlation with chlorine ($r_{Cl/Ti}$= 0.93), while Si shows no correlations. The correlation between Ti and Cl may indicate a common origin from sea-water. Moreover, Fe and Zn are well correlated in this fraction ($r_{Fe/Zn}$ = 0.95). In the coarse fraction, Zn is commonly associated with tire wear and iron can be related to brake wear emissions (Thorpe and Harrison, 2008).

239 *3.2 Enrichment Factors (EFs)*

240 Crustal enrichment factors (EFs_{cru}) were calculated for TSP and for each element in each mode
241 using silicon as a reference for the average crustal composition (Rudnick and Gao, 2004) with the
242 aim of highlighting the different origin of analyzed elements. On TSP, several elements (Cl, S, V,
243 Cr, Ni, Cu, and Zn) show $EFs_{cru} >> 100$ and are considered anomalously enriched elements (Chester,
244 2000). These elements have a non-crustal origin, i.e. marine (Cl) and anthropogenic (Cu, Zn, S, Cr,
245 Ni). Conversely, typical crustal elements (Al, Ca, Ti and Fe) show $EFs_{cru} < 10$, indicating common
246 origins from the lithosphere. EFs_{cru} of sodium, magnesium, potassium and manganese ranging from
247 49 (Na) to 22 (Mg) show that these elements are slightly enriched and suggest that a fraction of the
248 elements consists of non-crustal sources. Among the three modes, these elements show the highest
249 EFs_{cru} in the submicrometric ($EF_{cru}(Na)= 67$; $EF_{cru}(Mg)= 29$; $EF_{cru}(K)= 88$; $EF_{cru}(Mn)= 64$) and the
250 lowest in the coarse ($EF_{cru}(Na)= 25$; $EF_{cru}(Mg)= 14$; $EF_{cru}(K)= 4$) and intermediate modes
251 ($EF_{cru}(Mn)= 13$). On this basis, the finest particles have a non-crustal origin (i.e. K from combustion
252 processes; Mn from road traffic; Na from marine aerosol), whereas coarse particle origin can be
253 mainly attributed to dust resuspension.

254 Marine influence on some elemental concentrations (Na, Mg, S, K, Ca) has been evaluated
255 calculating the sea-water enrichment factors (EFs_{sea}) using chlorine as reference for the average sea-
256 water composition (Millero et al., 2008) (Table SI4). Chlorine was preferred to sodium because: (i)
257 it is not affected by PIXE X-ray self-absorption; (ii) previous source apportionment studies in the
258 area (Masiol et al., 2012a) pointed out its better role as sea-salt tracer and (iii) the supposed limited
259 chlorine depletion due to the low levels of atmospheric oxidants normally recorded in the coldest
260 seasons. Na and Mg show low sea EFs_{sea} in all modes indicating a probable origin from sea-water.
261 Sulfur and potassium (in the intermediate and coarse modes) and Ca (in all modes) are slightly
262 enriched and suggest that a significant fraction of the elements was of non-marine source. On the
263 contrary, sulfur and potassium show $EFs_{sea} >> 100$ in the submicrometric modes indicating a non-
264 marine source.

265

266 *3.3 Relationships between elemental mass size distributions and atmospheric circulation*

267 *3.3.1 Cluster analysis on back-trajectories*

268 Daily back-trajectories were computed and a cluster analysis was applied using HYSPLIT. The
269 appropriate number of clusters was set to 4 on the basis of total spatial variance analysis
270 corresponding to: (1) Central and Eastern Europe (N=2); (2) the Adriatic Sea (N=5); (3) the Arctic
271 (N=5); and, (4) the North Atlantic (N=2) directions. The average back-trajectories associated to

each cluster are reported in Figure 1c, while the average elemental concentrations for each group are listed in Table 1.

Most polluted samples are grouped in days characterized by air masses coming from Central and Eastern Europe directions. These samples show an increase of Na, Mg, Al, S, Cl, K, Ca, Ti Mn, Ni, Cu and Zn mainly in the intermediate mode. In the submicrometric mode, high concentrations of sulfur have been observed in group 2 (the Adriatic Sea) and 3 (the Arctic), while Cl, Fe and Zn show an increase in group 4 (the North Atlantic). Silicon increases in the coarse mode when air masses came from the Adriatic Sea. Days characterized by air masses coming from the North Atlantic direction showed a drop in the average concentrations of Al, S and Cl. These results confirm what has been previously observed in Masiol et al. (2012a) and, that: (i) pollution-related elements, and consequently the component of their emission sources, increase when air masses come from Central-Eastern Europe direction; (ii) crustal and sea-related elements increased when air masses passed over the Adriatic Sea and (iii) air masses from Northern Europe direction generally were less pollutant loaded. Moreover, it can be seen that long-range transports mainly affect the submicrometric and intermediate modes including mostly pollution-related elements while, except for silicon, the coarse mode appears only slightly influenced by air mass origin.

3.3.2 Cluster analysis on wind data

Subsequently, the studied samples were grouped on the basis of surface wind speed and direction following the procedure described in Darby (2005) and using daily-averaged data. Days were clustered in 4 groups. V and Cr showed no significant differences among groups and were not considered in this discussion. Group 1 (N = 4) links days were characterized by moderate wind speeds (1.6 m s^{-1}), absence of wind calm in a NNE direction. In these conditions, an increase of Na, Mg and Al in the submicrometric mode and Ti in the intermediate mode, while not representing the main modes for these elements, were observed (Fig. 3).

Group 2 was composed of 1 day showing high wind speed (3.2 m s^{-1}) and no wind calm hours. Strong winds from northeast and east (coastline direction) likely favored the formation of sea-spray. In these conditions, sea-salt aerosol is primarily generated on the sea surface by bubble bursting when waves break due to wind stress. Moreover, it is heavily dependent on wind speed, as from approximately 3-4 m s^{-1} (O'Dowd et al., 1997). A high concentration of Cl was also observed in the intermediate mode. Other elements showed the lowest concentrations in each mode excepting silicon which presented high concentrations in the coarse mode. This could have been due to the resuspension of fine sand particles from the nearby beach. However, the injection of crustal particles together with sea spray due to the wave breaks cannot be excluded.

Group 3 (N = 2) and group 4 (N = 7) presented similar average wind speed (0.8 m s^{-1}) and high percentage of wind calm hours (13% and 17%, respectively), but different prevailing wind direction. Group 3 linked days with prevailing winds from WSW (from the Adriatic Sea) resulting in incoming clean air and thus lower elemental concentrations with respect to groups 1 and 4. Group 4 depicted wind blowing from NWN-N-NE (from Venice city and the mainland) in conditions of low wind speed and high percentage of wind calm hours, that favored the accumulation of S, K, Ca, Mn, Fe, Ni, Cu and Zn in the submicrometric and intermediate modes. On this basis and considering background information about PM sources, these elements represented the markers of mainland emissions such as combustion processes (S, K), construction works in the proximity of the sampling site (Ca), traffic or industrial processes (Fe, Ni, Cu and Zn), such as emissions from the glass-making factories on the island of Murano (Rampazzo et al., 2008b).

In this view, long-range transports and local weather conditions were mainly seen to affect the elemental concentrations in the intermediate and submicrometric modes causing an increase or, vice versa, a decrease of elements related to several anthropogenic sources.

Conclusion

Mass size distributions of selected elemental tracers were investigated in a semi-rural coastal site near Venice (Italy). From the experimental data information was obtained on potential pollutant sources by investigating the relationships between elements in the different size fractions. An approach to detect the importance of local atmospheric circulation and air mass origin in the PM composition and fractional distribution is suggested.

An increase in pollution-related elements (S, Ca, K, Fe, Ni, Cu and Zn) in the submicrometric and intermediate mode was observed when air masses came from Central and Eastern Europe direction. Moreover, wind blowing from NWN-N-NE (from Venice mainland) with low wind speed and high percentage of wind calm hours favored their accumulation. These elements could be also considered as markers of mainland emissions such as combustion processes (S, K), construction works (Ca) and traffic (Fe, Ni, Cu and Zn). As the size of particles also determines how deep in the respiratory tract aerosol is inhaled, these results highlighted that anthropogenic emitted PM was mainly present in the finest fraction, evidencing associated potential health consequences on the population. And, finally, levels strongly depended on air mass origin and local meteorological conditions.

Despite the limited number of processed data, the methodological approach used to identify the sources of elements may be easily applicable in different atmospheric scenarios and be of interest for the scientific community.

Acknowledgements

This study presents a part of a PhD thesis of Mauro Masiol, financed by the Italian Ministry of Education, University and Research (MIUR). The authors are grateful to INFN − Legnaro laboratories (http://www.lnl.infn.it) for PIXE, ARPAV – Centro Meteorologico di Teolo for weather data and Comando Zona Fari e Segnalamenti Marittimi di Venezia for logistics. The authors gratefully acknowledge the NOAA Air Resources Laboratory (ARL) for the provision of the HYSPLIT transport and dispersion model and READY website (http://ready.arl.noaa.gov) used in this publication.

References

Amato, F., Pandolfi, M., Moreno, T., Furger, M., Pey, J., Alastuey, A., Bukowiecki, N., Prevot, A.S.H., Baltensperger, U., Querol, X., 2011. Sources and variability of inhalable road dust particles in three European cities. Atmos. Environ. 45, 6777-6787.

ARPAV (Environmental Protection Agency of Veneto Region), 2013. Regional relation of air quality - Year 2012, pp. 85 [in Italian]. Available from: http://www.arpa.veneto.it/temi-ambientali/aria/file-e-allegati/documenti/relazioni-regionali-della-qualita-dellaria/RELAZIONE%20ANNUALE%20QA%202012_rev0.0.pdf.

Benson, D.R., Yu, J.H., Markovich, A., Lee, S.H., 2011. Ternary homogeneous nucleation of H_2SO_4, NH_3, and H_2O under conditions relevant to the lower troposphere. Atmos. Chem. Phys. 11(10), 4755-4766.

Buseck, P.R., Schwartz, S.E., 2003. Tropospheric aerosols. In: Turekian, K.K., Holland, H.D. (eds), Treatise on Geochemistry, volume 4. Elsevier Science Ltd, San Diego, pp 91-142.

Chester, R.., 2000. Marine Geochemistry. Blackwell Science, Oxford, 506 pp.

Chow, J.C., Bachmann, J.D., Wierman, S.S.G., Mathai, C.V., Malm, W.C., White, W.H., Mueller, P.K., Kumar, N., Watson, J.G., 2002. Visibility: Science and Regulation. J. Air Waste Ma 52 (9), 973-999.

Contini, D., Gambaro, A., Belosi, F., De Pieri, S., Cairns, W.R.L., Donateo, A., Zanotto, E., Citron, M., 2011. The direct influence of ship traffic on atmospheric PM2.5, PM10 and PAH in Venice. J. Environ. Manage. 92, 2119-2129.

Darby L., 2005. Cluster analysis of surface winds in Houston, Texas, and the impact of wind patterns on ozone. J. Appl. Meteorol. 44, 1788-1806.

Draxler R.R., Rolph G.D., 2013. HYSPLIT (HYbrid Single-Particle Lagrangian Integrated Trajectory) Model access via NOAA ARL READY Website

(http://ready.arl.noaa.gov/HYSPLIT.php). Silver Spring, MD: NOAA Air Resources Laboratory.

EEA (European Environment Agency), 2013. AirBase: a Public Air Quality Database. http://www.eea.europa.eu/themes/air/airbase (last accessed June, 2013).

George I.J., Abbatt, J.P.D. 2010. Heterogeneous oxidation of atmospheric aerosol particles by gas-phase radicals. Nature Chemistry 2, 713-722.

Karanasiou, A. A., Sitaras, I. E., Siskos, P. A., Eleftheriadis, K., 2007. Size distribution and sources of trace metals and n-alkanes in the Athens urban aerosol during summer. Atmos. Environ. 41, 2368-2381.

Kroll, J.H., Seinfeld, J.H., 2008. Chemistry of secondary organic aerosol: Formation and evolution of low-volatility organics in the atmosphere. Atmos. Environ. 42, 3593-3624.

Lewis, E.R., Schwartz, S.E., 2004. Sea Salt Aerosol Production. Mechanisms, Methods, Measurements, and Models. Geophysical Monograph 152. American Geophysical Union, Washington DC, 413 pp.

Lohmann, U., Feichter J., 2005. Global indirect aerosol effects: a review. Atmos. Chem. Phys. 5, 715-737.

Majoral, C., Le Pape, A., Diot, P., Vecellio, L., 2006. Comparison of various methods for processing cascade impactor data. Aerosol Sci. Tech. 40 (9), 672-682.

Masiol, M., Rampazzo, G., Ceccato, D., Squizzato, S., Pavoni, B., 2010. Characterization of PM10 sources in a coastal area near Venice (Italy): an application of factor-cluster analysis. Chemosphere 80, 771-778.

Masiol, M., Squizzato, S., Ceccato, D., Rampazzo, G., Pavoni, B., 2012a. Determining the influence of different atmospheric circulation patterns on PM_{10} chemical composition in a source apportionment study. Atmos. Environ. 63, 117-124.

Masiol, M., Squizzato, S., Ceccato, D., Rampazzo, G., Pavoni, B., 2012b. A chemometric approach to determine local and regional sources of PM10 and its geochemical composition in a coastal area. Atmos. Enviro. 54, 127-133.

Maxwell, J.A., Teesdale, W.J., Campbell J.L., 1995. The Guelph PIXE package II. Nucl. Instrum. Method B 95, 407-421.

Millero, F. J., Feistel, R., Wright, D. G., McDougall, T. J., 2008. The composition of Standard Seawater and the definition of the Reference-Composition Salinity Scale. Deep-Sea Res PT I 55, 50-72.

405 Moldanová, J., Fridella, E., Popovicheva, O., Demirdjian, B., Tishkova, V., Faccinetto, A., Focsa,
406 C., 2009. Characterisation of particulate matter and gaseous emissions from a large ship
407 diesel engine. Atmos. Environ. 43, 2632-2641.
408 Moreno, T., Querol, X., Alastuey, A., de la Rosa, J., Sánchez de la Campa, A.M., Minguillón, M.,
409 Pandolfi, M., González-Castanedo, Y., Gibbons, W., 2010. Variations in vanadium, nickel
410 and lanthanoid element concentrations in urban air. Sci. Total Environ. 408 (20), 4569-
411 4579.
412 Ning, Z., Sioutas C., 2010. Atmospheric processes influencing aerosols generated by combustion
413 and the inference of their impact on public exposure: a review. Aerosol Air Qual.Res. 10
414 (1), 43-58.
415 O'Dowd, C.D., Smith, M.H., Consterdine, I.E., Lowe, J.A., 1997. Marine aerosol, sea-salt, and the
416 marine sulphur cycle: a short review. Atmos. Environ. 31, 73-80.
417 Pant, P., Harrison, R.M., 2013. Estimation of the contribution of road traffic emissions to particulate
418 matter concentrations from field measurements: A review. Atmos. Environ. 77, 78-97.
419 Pope, C.A. III, Ezzati, M., Dockery, D.W., 2009. Fine-particulate air pollution and life expectancy
420 in the United States. New Engl. J. Med., 360, 376-386.
421 Rampazzo, G., Masiol, M., Visin, F., Pavoni, B., 2008a. Gaseous and PM10-bound pollutants
422 monitored in three environmental conditions in the Venice area (Italy). Water Air Soil Poll.
423 195, 161-176.
424 Rampazzo, G., Masiol, M., Visin, F., Rampado, E., Pavoni, B., 2008b. Geochemical characterization
425 of PM10 emitted by glass factories in Murano, Venice (Italy). Chemosphere 71, 2068-
426 2075.
427 Rizzio E., Giaveri, G., Arginelli, D., Gini, L., Profumo, A., Gallorini, M., 1999. Trace elements total
428 content and particles-size distribution in the air parti culate matter of a rural-residentatial
429 area in north Italy investigated by instrumental neutron activation analysis. Sci. Total
430 Environ. 226, 47-56.
431 Rolph G.D., 2013. Real-time Environmental Applications and Display sYstem (READY) Website
432 (http://ready.arl.noaa.gov). Silver Spring, MD: NOAA Air Resources Laboratory.
433 Rudnick, R.L., Gao, S., 2004.Composition of the continental crust, in: R.L. Rudnick (Ed.), Treatise
434 on Geochemistry, The Crust, vol. 3, Elsevier, Amsterdam, pp. 1-64
435 Saarnio, K., Aurela, M., Timonen, H., Saarikoski, S., Teinila, K., Makela, T., Sofiev, M., Koskinen,
436 J., Aalto, P.P., Kulmala, M., Kukkonen, J., Hillamo, R., 2010. Chemical composition of
437 fine particles in fresh smoke plumes from boreal wild-land fires in Europe. Sci. Total
438 Environ. 408, 2527-2542.

Salma, I., Maenhaut, W., Záray, G., 2002. Comparative study of elemental mass size distributions in urban atmospheric aerosol. J. Aerosol Sci. 33, 339-356.

Samara, C., Voutsa, D., 2005. Size distribution of airborne particulate matter and associated heavy metals in the roadsite environment. Chemosphere 59, 1197-1206.

Seinfeld, J.H., Pandis, S.N., 2006. Atmospheric Chemistry and Physics: From Air Pollution to Climate Change, second ed. Wiley-Interscience, Hoboken, 1203 pp.

Squizzato, S., Masiol, M., Innocente, E., Pecorari, E., Rampazzo, G., Pavoni, B., 2012. A procedure to assess local and long-range transport contributions to PM2.5 and secondary inorganic aerosol. J. Aerosol Sci. 46, 64-76.

Squizzato, S., Masiol, M., Brunelli, A., Pistollato, S., Tarabotti, E., Rampazzo, G., Pavoni, B. 2013. Factors determining the formation of secondary inorganic aerosol: a case study in the Po Valley (Italy). Atmos. Chem. Phys. 13, 1927-1939.

Sternbeck, J., Sjodin, A., Andreason, K., 2002. Metal emissions from road traffic and the influence of resuspension: results from two tunnel studies. Atmos. Environ. 36, 4735-4744.

Thorpe, A., Harrison, R.M, 2008. Sources and properties of non-exhaust particulate matter from road traffic: A review. Sci. Total Environ. 400, 270-282.

Toscano G., Moret I., Gambaro A., Barbante C.,. Capodaglio G., 2011. Distribution and seasonal variability of trace elements in atmospheric particulate in the Venice Lagoon. Chemosphere 85, 1518-1524.

Yu H., Kaufman, Y.J., Chin, M., Feingold, G., Remer, L.A., Anderson, T.L., Balkanski, Y., Bellouin, N., Boucher, O., Christopher, S., DeCola, P., Kahn, R., Koch, D., Loeb, N., Reddy, M.S., Schulz, M., Takemura, T., Zhou, M., 2005. A review of measurement-based assessment of aerosol direct radiative effect and forcing. Atmos. Chem. Phys. 5, 7647-7768.

Table caption

Table 1. Mean concentration (in ng m^{-3}) measured for each fraction and for each back-trajectories cluster.

Table 1
Click here to download Table: Table 1.doc

Table 1. Mean concentration (in ng m^{-3}) measured for each fraction and for each back trajectories cluster. Valid data (>DL) on which the mean is calculated are reported in round brackets for each values.

	Submicrometric	Intermediate	Coarse	Submicrometric			Intermediate				Coarse				
ng m^{-3}	< 1 µm	1 − 4 µm	> 4 µm	Central and Eastern Europe	Adriatic Sea	Arctic	North Atlantic	Central and Eastern Europe	Adriatic Sea	Arctic	North Atlantic	Central and Eastern Europe	Adriatic Sea	Arctic	North Atlantic
Na	277.0 (3)	379.8 (7)	589.9 (2)	<DL	203.4 (1)	313.8 (2)	<DL	1345.9 (1)	318.2 (3)	119.3 (3)	<DL	<DL	<DL	589.0 (2)	<DL
Mg	123.6 (5)	200.1 (5)	225.5 (3)	<DL	113.8 (3)	138.4 (1)	<DL	793.8 (1)	77.3 (2)	26.0 (2)	<DL	<DL	53.9 (1)	331.6 (1)	291.1 (1)
Al	115.6 (5)	80.2 (6)	80.4 (4)	<DL	136.6 (2)	135.6 (2)	33.6 (1)	251.6 (1)	51.8 (2)	52.2 (2)	21.9 (1)	<DL	42.7 (2)	118.2 (2)	<DL
Si	50.8 (13)	69.6 (10)	197.8 (5)	52.7 (2)	35.1 (5)	67.8 (5)	40.6 (1)	123.8 (2)	64.3 (2)	42.3 (4)	86.0 (1)	37.9 (1)	448.6 (1)	26.8 (2)	<DL
S	745.4 (14)	249.6 (11)	38.2 (8)	575.6 (2)	789.2 (5)	832.9 (5)	586.8 (2)	1874.3 (1)	97.3 (5)	89.5 (3)	57.9 (2)	26.1 (1)	47.8 (3)	32.4 (3)	29.2 (1)
Cl	49.0 (12)	623.0 (13)	103.7 (9)	13.7 (2)	73.9 (4)	8.7 (5)	220.8 (1)	3660.2 (1)	469.5 (5)	353.8 (5)	160.9 (2)	100.1 (1)	80.5 (4)	131.9 (3)	64.1 (1)
K	260.0 (14)	68.1 (14)	10.1 (12)	162.7 (2)	240.5 (5)	261.9 (5)	401.5 (2)	283.9 (2)	35.2 (5)	29.5 (5)	31.0 (2)	11.4 (1)	9.1 (5)	8.9 (4)	14.4 (2)
Ca	39.0 (14)	214.1 (14)	39.0 (10)	41.2 (2)	45.3 (5)	32.5 (5)	37.2 (2)	891.1 (2)	110.2 (5)	67.5 (5)	163.3 (2)	25.5 (2)	41.1 (3)	48.9 (3)	34.4 (2)
Ti	3.1 (8)	9.2 (8)	8.3 (7)	3.9 (1)	4.4 (2)	2.8 (3)	1.9 (2)	39.6 (1)	3.5 (3)	8.4 (2)	3.2 (2)	<DL	2.0 (4)	16.8 (3)	<DL
V	3.1 (7)	0.2 (1)	<DL	2.7 (1)	3.2 (3)	2.7 (2)	4.3 (1)	<DL	<DL	0.2 (1)	<DL	<DL	<DL	<LOD	<DL
Cr	5.9 (11)	3.2 (7)	10.1 (4)	4.5 (2)	4.8 (3)	8.3 (4)	4.2 (2)	1.6 (1)	2.2 (2)	4.6 (3)	2.7 (1)	<DL	6.2 (1)	22.4 (1)	5.9 (2)
Mn	6.8 (11)	3.1 (8)	0.7 (4)	4.1 (2)	7.1 (3)	6.5 (4)	9.7 (2)	11.9 (1)	2.0 (3)	1.2 (3)	3.1 (1)	0.8 (1)	0.7 (2)	0.4 (1)	<DL
Fe	66.5 (14)	53.7 (14)	12.7 (12)	53.7 (2)	57.3 (5)	59.9 (5)	119.1 (2)	44.1 (2)	58.1 (5)	29.1 (5)	113.8 (2)	19.4 (2)	8.2 (5)	14.7 (4)	13.5. (1)
Ni	3.0 (9)	12.6 (6)	1.1 (6)	1.2 (1)	2.0 (3)	4.7 (3)	3.0 (2)	48.6 (1)	0.9 (2)	12.0 (2)	1.2 (1)	1.2 (1)	0.9 (1)	1.1 (4)	<DL
Cu	3.9 (12)	27.2 (9)	1.3 (5)	1.7 (2)	4.1 (4)	3.7 (4)	6.2 (2)	109.8 (2)	3.1 (3)	2.6 (3)	8.0 (1)	1.9 (1)	1.2 (1)	1.0 (2)	1.5 (1)
Zn	38.8 (13)	49.8 (8)	3.2 (7)	20.1 (2)	29.3 (5)	39.7 (4)	79.3 (2)	286.8 (1)	12.5 (3)	15.2 (2)	21.8 (2)	12.0 (1)	2.3 (3)	1.2 (2)	1.2 (1)

Figure 1

Click here to download high resolution image

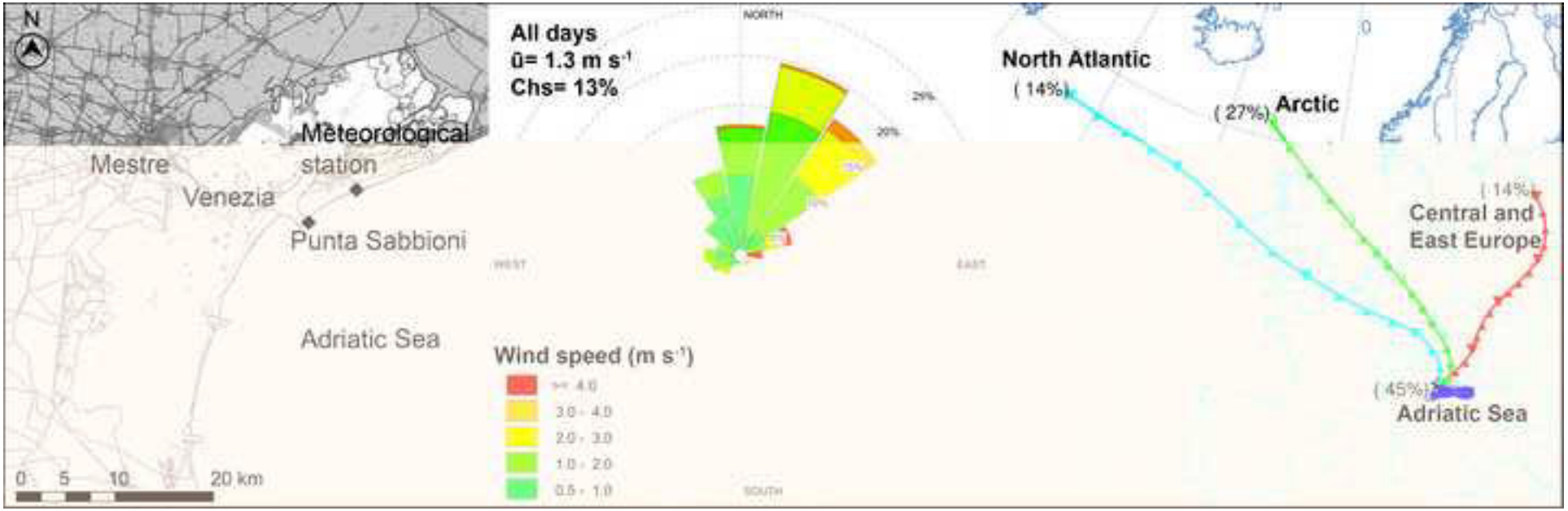

Figure 2

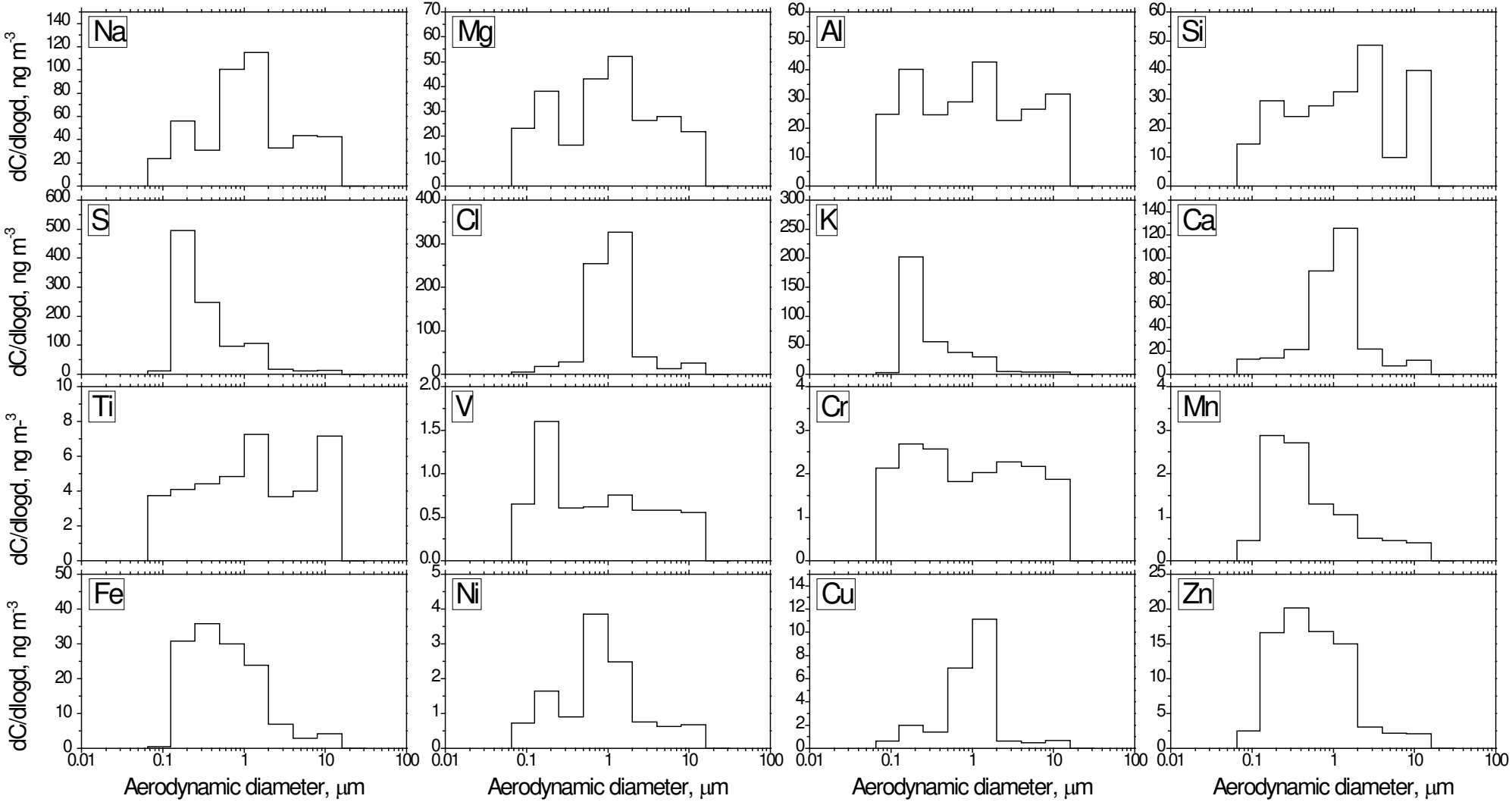
Na
Mg
Al
Si
S
Cl
K
Ca
Ti
V
Cr
Mn
Fe
Ni
Cu
Zn
dC/dlogd, ng m-3
Aerodynamic diameter, μm
0.01
0.1
1
10
100

Figure 3

Group 1
ū= 1.6 m s^{-1}
Chs= 0%

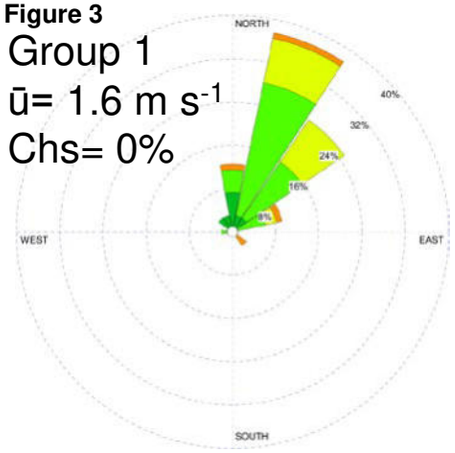

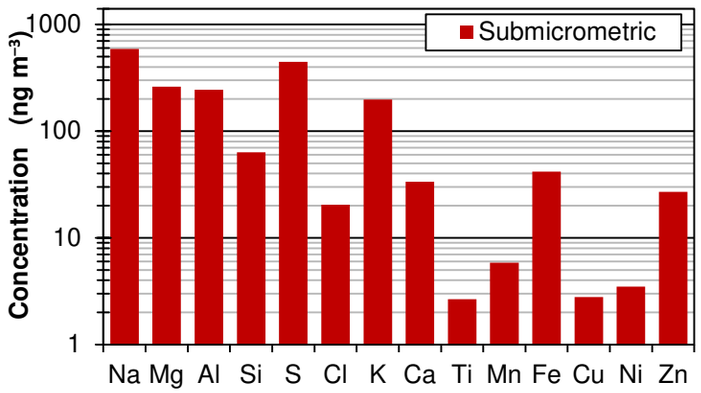

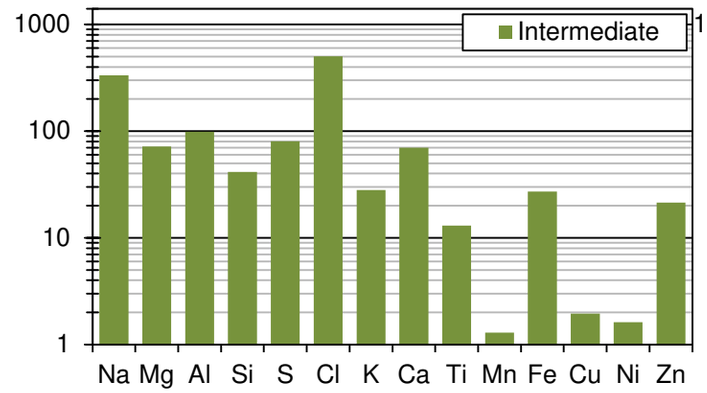

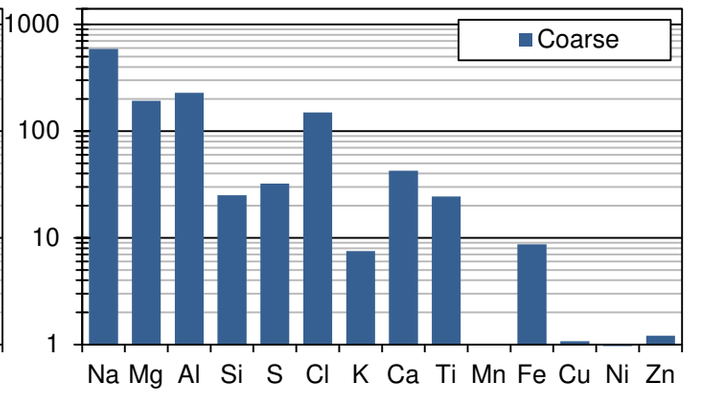

Group 2
ū= 3.2 m s^{-1}
Chs= 0%

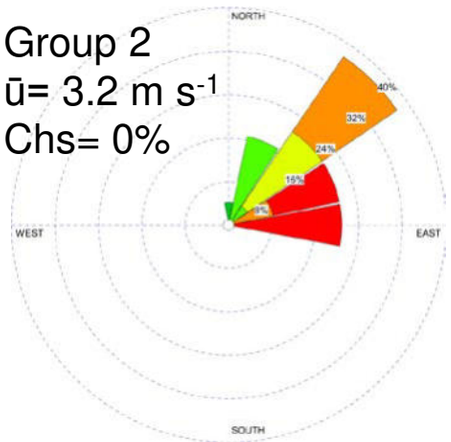

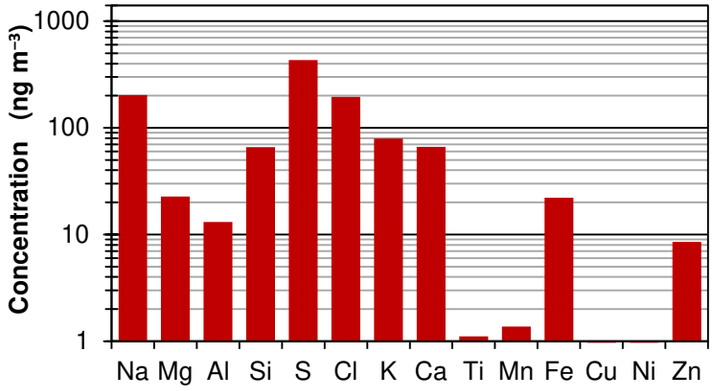

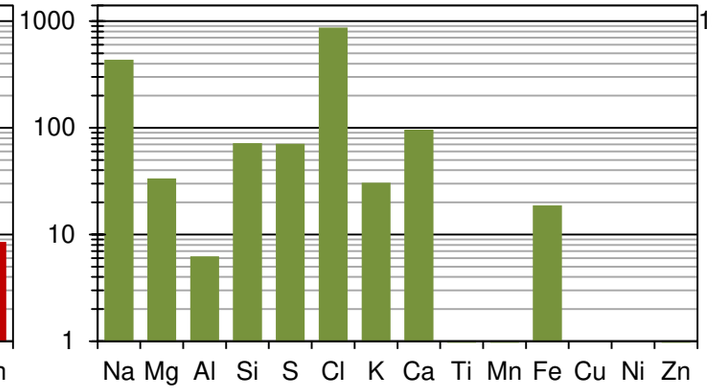

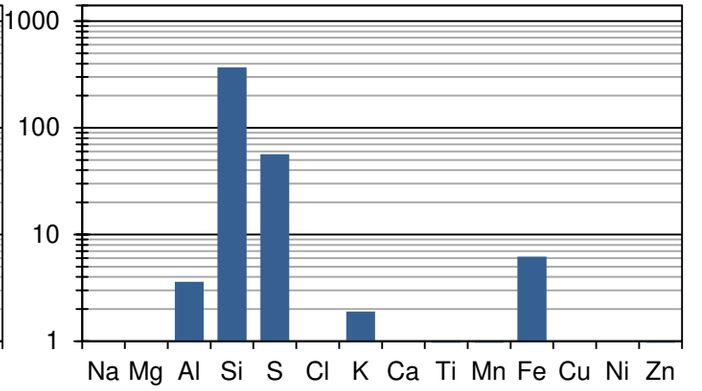

Group 3
ū= 0.8 m s^{-1}
Chs= 13%

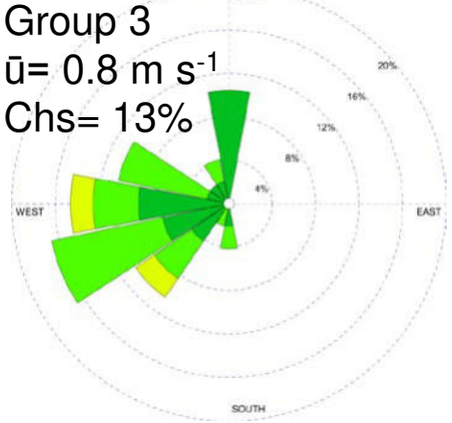

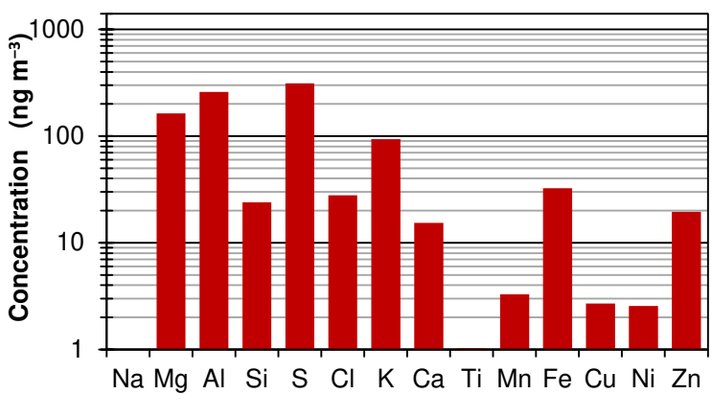

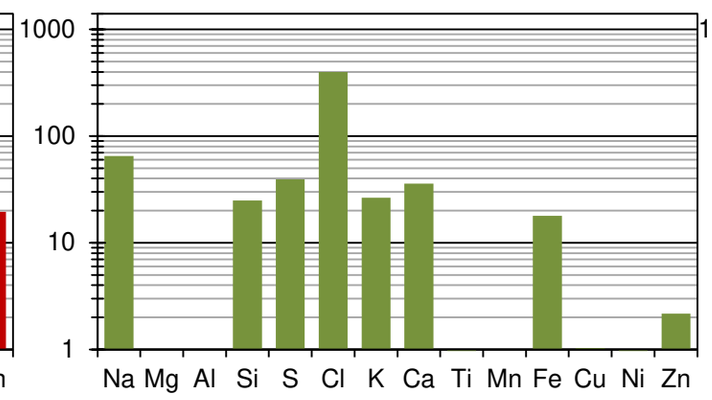

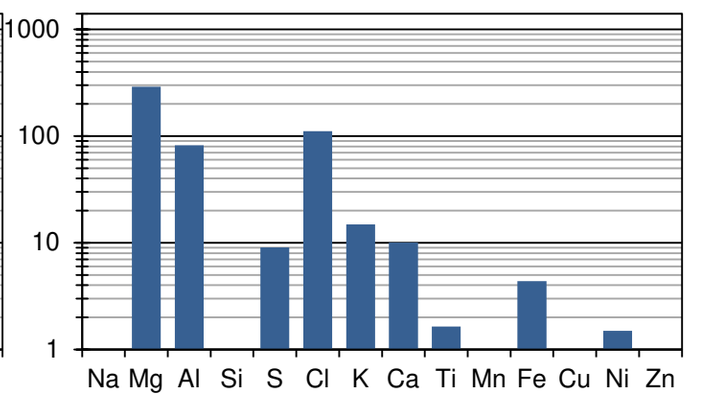

Group 4
ū= 0.8 m s^{-1}
Chs= 17%

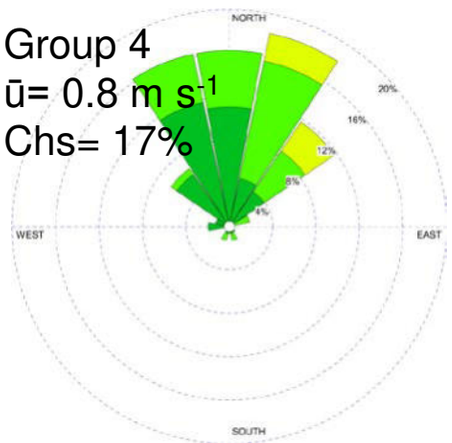

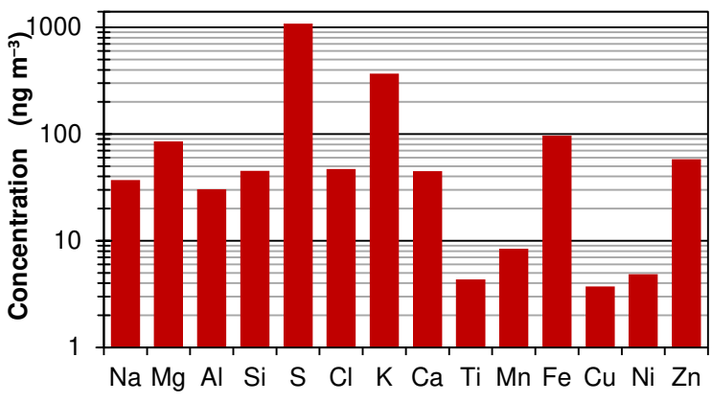

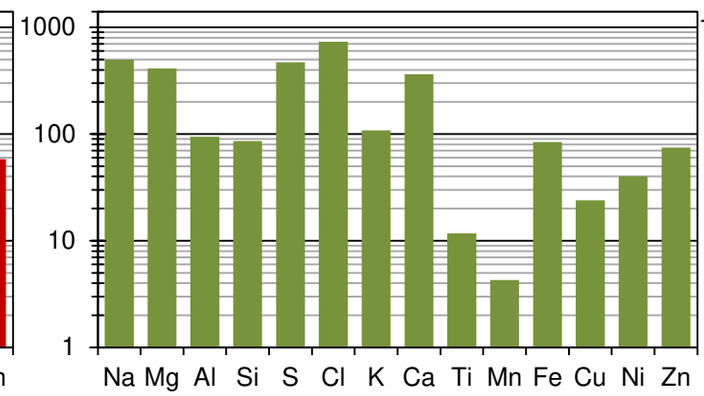

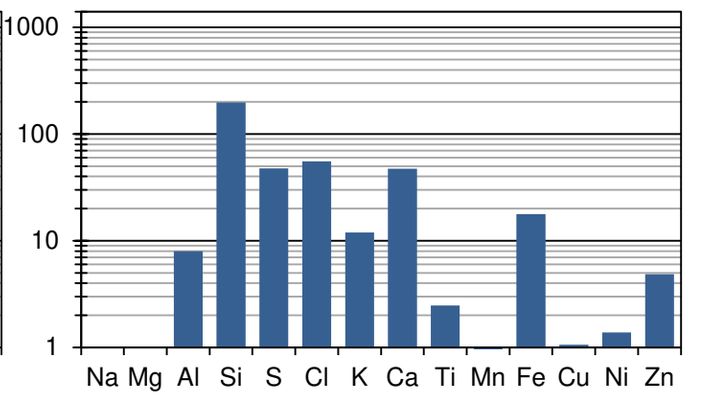

Wind speed (m s^{-1}): > 4.0 | 3.0 – 4.0 | 2.0 – 3.0 | 1.0 – 2.0 | 0.5 – 1.0

Figure captions

Figure 1. Map of the study area, wind rose calculated for the sampling period and back-trajectories clusters. In the wind rose: ū represents the average wind speed and Chs the percentage of wind calm hours.

Figure 2. Elements size distribution expresses as differential mass concentration.

Figure 3. Wind roses calculated for each identified group and average concentration of elements in each mode (in logarithmic scale) (ū represents the average wind speed and Chs the percentage of wind calm hours).